Supplemental data

The intrinsically low open probability of α7 nAChR can be overcome by positive allosteric modulation and serum factors leading to the generation of excitotoxic currents at physiological temperatures.

Dustin K. Williams, Can Peng, Matthew R. Kimbrell, and Roger L. Papke

Molecular Pharmacology

Supplemental Materials and Methods

Generation of HEK 293 cells stably expressing human α7 and human RIC-3

Low passage number HEK 293 cells were obtained from American Type Culture Collection (Manassas, VA). The cells were routinely cultured in Dulbecco's modified eagle medium (DMEM) supplemented with 10% fetal bovine serum (FBS). In order to create a HEK 293 cell line stably expressing human α7 and RIC-3, two rounds of stable transfection were performed. The transfections were performed with Fugene HD (Roche, Indianapolis IN) according to manufacturer's directions. The day before transfection, 125,000 cells were plated in 35 mm dishes. First, cells were transfected with 1 μg (per 35 mm dish) of circular pcDNA3.1 plasmid containing the RIC-3 gene. Several (>20) clones that were resistant to 0.15 mg/ml hygromycin (resistance conferred by pcDNA3.1/RIC-3 vector) after a two-week selection period were isolated using cloning cylinders and expanded. Following the selective period, the hygromycin-resistant cell lines were maintained in normal growth media supplemented with 0.15 mg/mL hygromycin. Total RNA was extracted using the SV Total RNA Isolation System (Promega, Madison, WI) and the expression of hRIC-3 mRNA was determined by reverse transcriptase-polymerase chain reaction (RT-PCR). The upper and lower primers for hRIC-3, respectively, were CCGATTTCCACCTATGATG and GGCTGCTTCTGTCTCCTTC, resulting in an expected product size of 346 base pairs. The upper and lower primers for glyceraldehyde-3-phosphate dehydrogenase (GAPDH), respectively, were ACGGATTTGGTCGTATTGG and TGGCATGGACTGTGGTCAT, resulting in an expected product size of 516 base pairs. RT-PCR products were visualized in gels composed of 0.7% agarose and 1.15%Synergel (Diversified Biotech, Dedham MA) . The process of transfection, selection, cloning, and expansion was repeated using a stable HEK-hRIC-3 expressing cell line as the starting point. The hRIC-3-expressing cell line was transfected with 2 μg of circular pCIneo/hα7 plasmid using Fugene HD (Roche, Indianapolis, IN). The cells were selected during a two-week period using 0.45 mg/mL geneticin and 0.015 mg/mL hygromycin, and thereafter maintained in the same concentration of selective antibiotics. Ten colonies were eventually cloned that were resistant to both hygromycin and geneticin that were also positive for both hRIC-3 and hα7 mRNA by RT-PCR. The upper and lower primers for hα7, respectively, were TGGACGTGGATGAGAAGAA and TTCCCACTAGGTCCCATTC, resulting in an expected product size of 414 base pairs. These cell lines were subsequently screened for functional α7 channel expression through whole-cell patch-clamp electrophysiology. The clone that showed highest functional channel expression and was easiest to patch-

clamp was selected for use in all of the following studies. This clone is referred to as the A7R3HC10 cell line for alpha7RIC-3-expressingHEK-derived Clone10. In addition, cell lines were also created stably expressing human α7 alone. HEK 293 cells were transfected with 2 μg of circular pCiNeo plasmid containing the human α7 gene. Cells were selected during a two-week period of exposure to 0.5 mg/mL geneticin (resistance conferred by pCiNeo/α7 vector), and thereafter were maintained in 0.5 mg/mL geneticin. None of the geneticin-resistant and PCR-positive clones for α7 alone responded to co-applications of ACh and PNU-120596 in patch-clamp electrophysiology experiments. However, responses from these cells were observed when cells stably expressing α7 were transiently transfected with hRIC-3 only (not shown). For normal passaging, cells were dissociated with a trypsin-free solution containing 0.02% EDTA in calcium- and magnesium-free Hank's balanced saline solution (HBSS) to avoid non-selective damage to the α7 nAChRs expressed on the cell surface. For electrophysiology experiments, cells were plated on poly-D-lysine-coated cover slips and were used 1-5 days after plating for experiments.

Immunoprecipitation and western blot

Three days prior to preparing the sample for western blotting, 50,000 cells were plated in a 12-well plate treated with poly-D-lysine. Cells were washed with ice cold 1% phosphate-buffered saline, lysed (lysis buffer, protease inhibitor, and phosphatase inhibitor), scraped off the 12- well plate, and transferred into 1.5 ml tubes. The cells were then sonicated on ice and incubated overnight at 4°C with primary antibody ab848, courtesy of Dr. Cecilia Gotti (University of Milan, Italy). The antigen-antibody complexes were incubated with 50 μl of pre-washed protein A magnetic beads (Millipore, Billerica, MA). After washing, immunoprecipitated protein underwent denaturing elution with sample buffer followed by heating to 80°C for 10 minutes. 40 μl were loaded into each well for SDS-polyacrylamide gel electrophoresis using 10% polyacrylamide, along with 1 μl of MagicMarkXP (Life Technologies, Grand Island, NY).

Protein was transferred overnight at 4°C onto a PVDF membrane. Transfer was confirmed by staining the PVDF membrane with Ponceau-S (Bio-Rad, Hercules, CA) and the gel with coomassie blue. Ponceau-S was removed from the membrane with TBS-T. The membrane was blocked at room temperature with 5% BSA. Overnight incubation at 4°C of the primary antibody ab849 (Dr. Cecilia Gotti) was followed by washing the membrane in TBS-T and incubating it with secondary antibody (Abcam, Cambridge, MA) for one hour at room temperature. After washing again with TBS-T,

Super Signal (Thermo Fisher Scientific, Waltham, MA) was added to visualize the protein using the ChemiXRS+ imaging system (Bio-Rad, Hercules, CA).

Fluorescence Microscopy

Untransfected HEK 293, A7R3HC10 (HEK-hα7/hRIC-3), HEK-hα7, and HEK-hRIC-3 cells were plated on square glass coverslips (Fisher Scientific, Waltham, MA) coated with poly-D-lysine and incubated at 37 °C with 5% CO_2 in DMEM media with 10% FBS containing the appropriate selective antibiotic for 24 hours prior to imaging. Cells were treated with 1 μg/mL (~125 nM) of Alexa488-α-btx (Life Technologies, Grand Island, NY) for 45 minutes at 37 °C with 5% CO_2. For a control, the A7R3HC10 cells were also pre-incubated with 1 mM nicotine, and then 1 μg/mL Alexa488-α-btx was co-applied with 1 mM nicotine. After the incubation, the cells were carefully rinsed 4 times with phosphate-buffered saline to remove any excess Alexa488-α-btx. The cells were then fixed with 4% (v/v) formaldehyde for 15 minutes, and washed 3 more times with phosphate-buffered saline before being mounted on coverslips for imaging using VectaShield (Vector Laboratories, Burlingame, CA) mounting media containing the nuclear stain DAPI. The slides were imaged immediately using an Olympus DSU-IX81 spinning disc confocal microscope. The images were obtained using a Hamamatsu C4742-80-12AG Monochrome CCD Camera.

Supplemental data

Generation and characterization of α7 expression in A7R3HC10 cells

Expression of hRIC-3 and hα7 mRNA in hygromycin- and geneticin- resistant clones

Total mRNA was isolated from each hygromycin- and geneticin-resistant clone and tested for the presence of hRIC-3 and hα7 mRNA through RT-PCR. As expected, untransfected HEK 293 were negative for hRIC-3 and for hα7, but bands corresponding to the expected nucleotide length were observed for both hRIC-3 and hα7 from the antibiotic-resistant cell lines (Supplemental Figure 1A). Messenger RNA for Glyceraldehyde 3-phosphate dehydrogenase, a common housekeeping gene, was probed as a positive control to verify that the RT-PCR protocol was successful in the case that hRIC-3 and hα7 bands were absent.

Identification of the hα7 protein via western blot in antibiotic- resistant clones

No labeling was observed from untransfected HEK 293 cells and cells stably expressing hRIC-3. In contrast, some labeling was observed from cells transfected with hα7 while stronger labeling was seen in cells stably expressing both hα7 and hRIC-3 (Supplemental Figure 1B). The α7 protein detected in this Blot is an aggregation with a molecular weight >220 kDa; the expected molecular weight of an α7 pentamer is 280 kDa.

Labeling of A7R3HC10 *cells with alexa488-conjugated α-btx*

Intact cells were labeled with Alexa488-conjugated α-btx to qualitatively verify surface expression of α7 nAChR and to illustrate the distribution of receptor expression in this cell line. As expected, the untransfected HEK 293, HEK-hα7, and A7R3HC10 cell lines were not labeled with the fluorescent toxin. In contrast, the A7R3HC10 cell line was labeled by the fluorescent α-btx, and in a competitive manner with 1 mM nicotine (Supplemental Figure 2). The labeling appears in non-continuous clusters, suggesting that surface expression of α7 in this cell line may be non-uniform. Similar non-continuous patterns of labeling by fluorescent dye-conjugated ligands of α7 have been seen in other cell lines and in cultured neurons (Hone et al., 2010; Valles et al., 2009).

MLA sensitive α7-mediated currents in A7R3HC10 cells

The ACh-evoked responses recorded from A7R3HC10 cells with patch-clamp electrophysiology were sensitive to inhibition by the α7-selective antagonist MLA in a concentration-dependent manner (Supplemental Figure 3). In this experiment, the ACh concentration was fixed at 170 μM (the EC_{50} for peak currents), with increasing co-applications of MLA. No pre-incubation with MLA was made in these experiments. The IC_{50} of MLA measured in this paradigm was 2.7±0.4 μM. Since chronic applications of MLA are often made at nanomolar concentrations to produce selective inhibition of a7 receptors, this may seem like a rather high value for MLA, but when one considers that IC_{50} values are dependent on variables such as agonist concentration, timing, and duration of antagonist applications, this value is reasonable. High affinity inhibition of α7-mediated responses is obtained only when MLA is pre-incubated prior to the application of agonist (Alkondon, 1992; Palma et al., 1996). In addition, the IC_{50} value of MLA in an oocyte experiment utilizing a similar protocol to the one used here (no MLA pre-incubation) was determined to be 1.2 ± 0.2 μM with an ACh concentration of 60 μM (Lopez-Hernandez et al., 2009). Given that the ACh concentration used here was 170

μM, or roughly 3-fold higher, the IC_{50} of 2.7±0.4 μM for MLA inhibition of responses evoked by 170 μM ACh is consistent with previously published data.

Calculation of the drug dilution factor for the pressure-application system

Drug solutions applied via the picospritzer system were previously determined to be diluted approximately 30-fold in experiments with hippocampal brain slices (Lopez-Hernandez et al., 2007). In this study, the picospritzer system was used in a similar manner to apply drugs, with the exception that drugs were applied to cultured cells rather than brain slices. In order to determine the effective dilution factor of drugs delivered to the cultured cells via picospritzer, shifts in the transmembrane potential were recorded by current-clamp as solutions with varying K^+ concentrations were applied to the cell. The shift in transmembrane potential was first determined when an external solution containing 50 mM K^+ was applied via bath perfusion. Then, test solutions containing various K^+ concentrations were applied to the cells via picospritzer, and comparisons were made to determine which concentration of K^+ applied via the picospritizer shifted the transmembrane potential most similarly to that observed when 50 mM K^+ was bath-perfused. Differences in osmolarity between experimental solutions were minimized by the addition of sucrose. The magnitude of the observed shift in transmembrane potential upon application of experimental K^+ solutions was dependent on the initial resting membrane of a cell; cells with resting potentials further away from the new equilibrium potential of K^+ showed larger shifts. As shown in Supplemental Figure 4, the relationship between resting membrane potential and depolarization was linear for a given K^+ concentration. The close correspondence between the 75 mM K^+ concentration in the drug delivery pipette and the 50 mM K^+ concentration delivered in the bath indicates that the effective dilution factor of solution applied via picospritzer in this study was 1.5. The dilution factor to cultured cells was expected to be smaller than with brain slices as the applied drug has to penetrate extracellular matrix/tissue layers to reach the neurons expressing the receptor of interest in brain slices. Based on this result, drug solutions were prepared that were 1.5-fold more concentrated than the desired final concentration when the picospritzer system was used. For example, 1.5 mM ACh was placed in the drug application pipette when 1 mM ACh was desired to be applied to the cell.

Apparent temperature-dependence of alpha7 positive allosteric modulators from whole-cell recordings

Although *in vivo* data with α7 PAMs are limited, the data that are available show that α7 PAMs produce effects when administered to living animals, suggesting that α7 PAMs work at physiological temperatures (reviewed in (Williams et al., 2011)). However, it has recently been reported that the potentiation of responses by the α7 PAMs PNU-120596 and SB-206553 may have a dependence on the temperature, with potentiation being drastically reduced near physiological temperatures (Sitzia et al., 2011). To investigate the effect of temperature on α7 PAM efficacy, we tested the activities of type I and type II PAMs at 37 ºC with whole-cell recordings from the HEK-hα7/hric3 cell line. The basic protocol used in these experiments was to obtain three responses at room temperature (23.5 °C), record three responses at 37 °C, and then reduce the temperature back down to 23.5 °C. Acetylcholine was co-applied with PAM for 3 seconds with 60-second inter-stimulus intervals. It is important to note that at 37 ºC the quality of the whole-cell seals usually decreased. Because of this, the parameters used to define an acceptable whole-cell recording at 37 ºC were more relaxed than they would be for a typical whole-cell recording made at room temperature. Whole-cell seals with access resistance <40 MΩ, input resistance >100 MΩ, and holding current <700 pA at 37 °C were included in the analysis. Prior to the increase in temperature, access resistances were <15 MΩ, input resistances were >1 GΩ, and the holding current was between -50 pA and 0 pA. In most cases, if the patch survived the time at 37 ºC, the whole-cell parameters improved as temperatures returned to room temperature. In rundown control experiments performed without temperature adjustments, the amplitude of the responses at the end of the experiment were ~70% of the responses at the beginning (Figure 6A-B).

When 1 mM ACh was applied without a PAM, peak currents at 37 °C were 47 ± 3% of the initial baseline currents recorded at 23.5 °C and they recovered to ~80% upon temperature reduction back to 23.5 °C, a full recovery based on the rundown control (Supplemental Figure 5C-D and Table 2). It is important to emphasize that in these experiments currents evoked by ACh alone were reduced by approximately 53% at 37 °C relative to 23.5 °C because when evaluating the effect of temperature on PAM potentiation the ACh-evoked responses recorded at 37 °C are used as the baseline for comparison. This observation confirms recent findings that responses evoked by ACh on α7 nAChR are reduced at 37 °C relative to room temperature (Jindrichova et al., 2012; Sitzia et al., 2011).

The potentiation of responses evoked by 100 μM ACh with either 1 mM 5-HI or 10 μM NS-1738, (both type I PAMs) at 37 °C was similar (Figure 7 and Table 2). With 1 mM 5HI potentiated responses were 33 ± 2% (67% reduction) and with 10 μM NS-1738

potentiated responses were 34 ± 5% (66% reduction) of the baseline responses at room temperature, both of which were significantly smaller than the reduction seen with ACh alone ($p<0.05$). In both cases the potentiated responses recovered when temperatures returned to 23.5 °C to an extent expected (~70-80%) based on the rundown control. Together, these results suggest that the ability of the type I PAMs to potentiate ACh-evoked responses may be reduced, but relatively conserved at physiological temperature.

Legends for Supplemental Figures

Supplemental Figure 1. Expression of human α7 and human RIC-3 by the A7R3HC10 cell line. A) Expression of hα7 and hRIC-3 mRNA is verified by RT-PCR. The observed bands for GAPDH, hα7, and hRIC-3 are 516 bp, 414 bp, and 346 bp, as expected for the primers used. B) Immunoprecipitation and western blot from cell lysates. Untransfected HEK 293 and hRIC-3 cells were negative for hα7 protein with hα7-alone cells being slightly positive, and A7R3HC10 cells being strongly positive. The labeled protein from HEK-hα7 and A7R3HC10 cell lysates is an aggregate with molecular weight > 220 kDa. The primary antibodies for α7 were generously provided by Dr. Cecilia Gotti (University of Milan, Italy).

Supplemental Figure 2. Labeling of intact A7R3HC10 cells with Alexa Fluor 488-α-btx. No labeling was observed for untransfected HEK 293, HEK-hRIC-3, or HEK-hα7 cell lines. In contrast, labeling was observed on A7R3HC10 cells in a competitive manner with 1 mM nicotine. Cellular nuclei are stained in blue with DAPI, and the Alexa Fluor 488-α-btx label is green.

Supplemental Figure 3. Inhibition of currents by MLA from A7R3HC10 cells. Inhibition of responses by MLA determined from peak responses. In these experiments increasing MLA concentrations were co-applied with 170 μM ACh, the EC_{50} for peak currents determined previously (Figure 1B). A) Each point represents the mean ± SEM determined from 4-6 cells. The holding potential was -70 mV. B) Representative traces illustrating the co-applied inhibition at varying concentrations of MLA compared to the control responses to 170 μM ACh.

Supplemental Figure 4. Determination of dilution factor in the pressure drug application system with cultured cells. Whole-cell current-clamp recordings were carried out while applying solutions containing various concentrations of KCl to A7R3HC10

cells. The relationship between the initial resting membrane potential and depolarization was linear for a given K^+ concentration (left panel). Shifts in the transmembrane potential when applying 75 mM KCl via picospritzer is most similar to those observed when applying 50 mM KCl via bath perfusion (right panel), suggesting that the dilution factor of the pressure application drug delivery system with cultured cells was 1.5.

Supplemental Figure 5. Agonist controls for whole-cell voltage-clamp recordings investigating the temperature effects of α7 PAMs. A & B) Rundown control performed at room temperature (n=15). A) Responses to the 3-second application of 1 mM ACh were recorded every 60 seconds and normalized to the maximum peak amplitude of each cell (black circles). B) Representative traces. C & D) Temperature-dependent effects of peak responses evoked by 1 mM ACh (n=7). C) Responses were normalized to the average peak amplitude recorded at 23.5 °C. Each data point is shown as the average normalized value ± SEM (black circles). Temperature is indicated by gray squares. D) Representative traces.

Supplemental Figure 6. Temperature dependence of alternative PAMs on potentiation of α7-mediated responses. Whole-cell currents from A7R3HC10 cells evoked by 3 second co-applications of ACh and PAM were recorded every 60 seconds with varied temperatures between 23.5 °C and 37 °C. A) Time course for 100 μM ACh and 1 mM 5-HI evoked peak responses (black circles, n=12). Temperature is indicated by gray squares. B) Representative traces of 100 μM ACh and 1 mM 5-HI evoked responses recorded at the indicated temperature. C) Time course for 100 μM ACh and 10 μM NS-1738 evoked peak responses (black circles, n=6). Temperature is indicated by gray squares. D) Representative traces of 100 μM ACh and 10 μM NS-1738 evoked responses recorded at the indicated temperature. Responses were normalized to the average peak amplitude of the three initial responses obtained at 23.5 °C. Each data point was represented as the average normalized value ± SEM. E) Time course for 100 μM ACh and 10 μM TQS evoked peak responses (black circles, n=7). Temperature is indicated by gray squares. F) Representative traces of 100 μM ACh and 10 μM TQS evoked responses recorded at the indicated temperature. The deterioration in whole-cell recording properties at 37 °C could lead to a reduction in the fidelity of the voltage-clamp. It is feasible that the currents evoked in the presence of PNU-120596, given their size, could contribute to a greater loss of voltage-clamp fidelity than may have occurred with ACh alone. However, the increased temperature had less effect on the responses evoked with TQS than on the responses evoked with PNU-120596, relative to their initial

baseline responses (46 ± 3% versus 12 ± 3%), despite the fact that the absolute magnitude of the responses recorded with TQS was larger than those with PNU-120596 (3,080 ± 484 pA versus 1,333 ± 414 pA at 23.5 °C and 1,438 ± 229 pA versus 104 ± 31 pA at 37 °C).

Supplemental References

Alkondon M, Pereira, E.F.R., Wonnacott, S., and Albuquerque, E.X. (1992) Blockade of nicotinic currents in hippocampal neurons defines methyllycaconitine as a potent and specific receptor antagonist. *Mol Pharmacol* **41**:802-808.

Hone AJ, Whiteaker P, Mohn JL, Jacob MH and McIntosh JM (2010) Alexa Fluor 546-ArIB[V11L;V16A] is a potent ligand for selectively labeling alpha 7 nicotinic acetylcholine receptors. *J Neurochem* **114**(4):994-1006.

Jindrichova M, Lansdell SJ and Millar NS (2012) Changes in temperature have opposing effects on current amplitude in alpha7 and alpha4beta2 nicotinic acetylcholine receptors. *PLoS One* **7**(2):e32073.

Lopez-Hernandez G, Placzek AN, Thinschmidt JS, Lestage P, Trocme-Thibierge C, Morain P and Papke RL (2007) Partial agonist and neuromodulatory activity of S 24795 for alpha7 nAChR responses of hippocampal interneurons. *Neuropharmacology* **53**(1):134-144.

Lopez-Hernandez GY, Thinschmidt JS, Zheng G, Zhang Z, Crooks PA, Dwoskin LP and Papke RL (2009) Selective inhibition of acetylcholine-evoked responses of alpha7 neuronal nicotinic acetylcholine receptors by novel tris- and tetrakis-azaaromatic quaternary ammonium antagonists. *Mol Pharmacol* **76**(3):652-666.

Palma E, Bertrand S, Binzoni T and Bertrand D (1996) Neuronal nicotinic alpha 7 receptor expressed in Xenopus oocytes presents five putative binding sites for methyllycaconitine. *J Physiol* **491**:151-161.

Sitzia F, Brown JT, Randall AD and Dunlop J (2011) Voltage- and Temperature-Dependent Allosteric Modulation of alpha7 Nicotinic Receptors by PNU120596. *Front Pharmacol* **2**:81.

Valles AS, Roccamo AM and Barrantes FJ (2009) Ric-3 chaperone-mediated stable cell-surface expression of the neuronal alpha7 nicotinic acetylcholine receptor in mammalian cells. *Acta Pharmacol Sin* **30**(6):818-827.

Williams DK, Wang J and Papke RL (2011) Positive allosteric modulators as an approach to nicotinic acetylcholine receptor-targeted therapeutics: Advantages and limitations. *Biochem Pharmacol* **82**(8):915-930.

Supplemental Figures

Figure S1

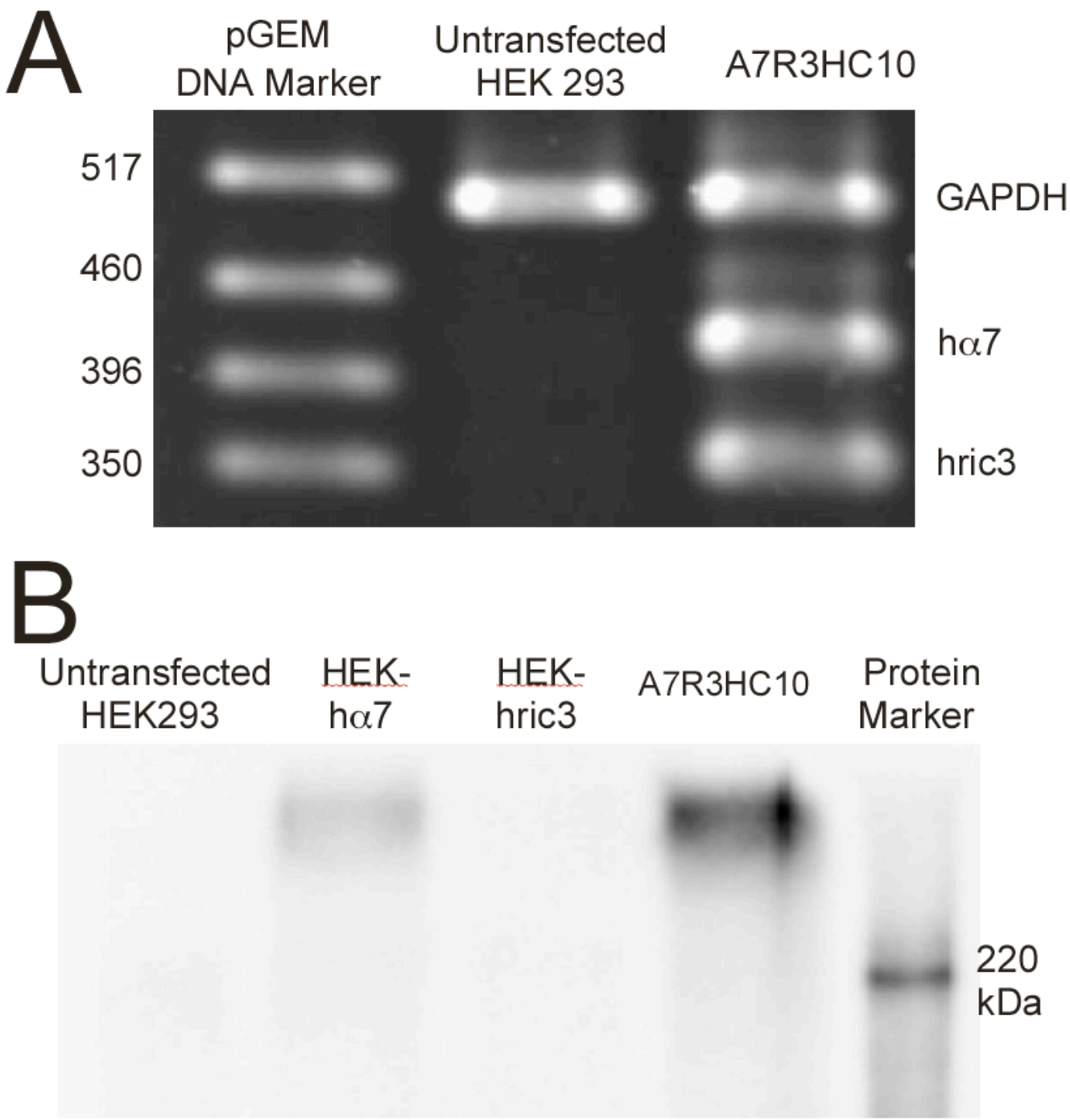
A
pGEM
DNA Marker
Untransfected
HEK 293
A7R3HC10
517
460
396
350
GAPDH
hα7
hric3
B
Untransfected
HEK293
HEK-
hα7
HEK-
hric3
A7R3HC10
Protein
Marker
220
kDa

Figure S2

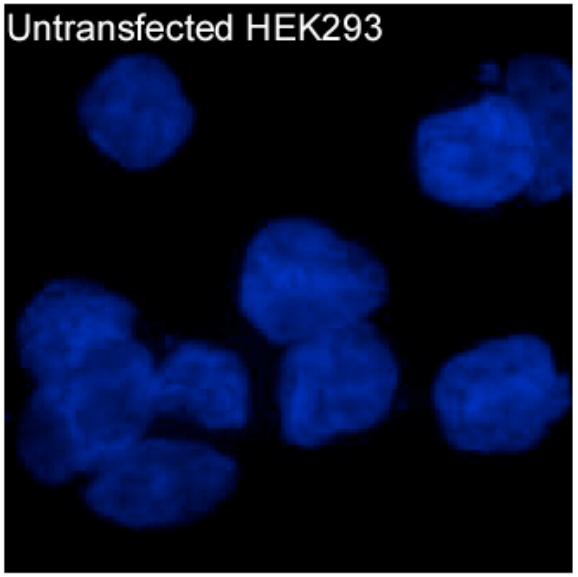
Untransfected HEK293

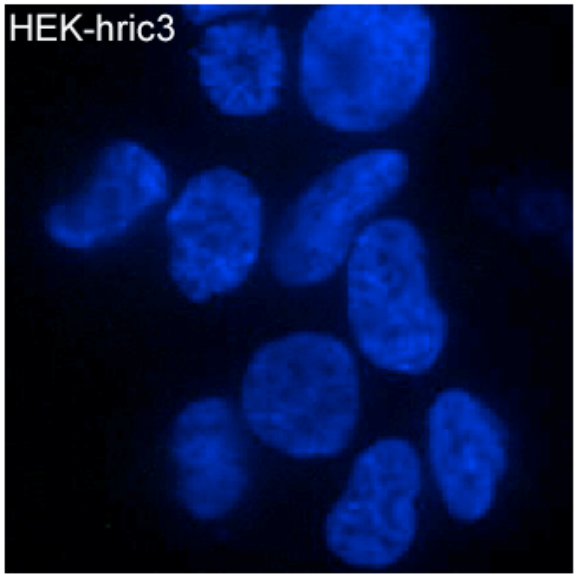
HEK-hric3

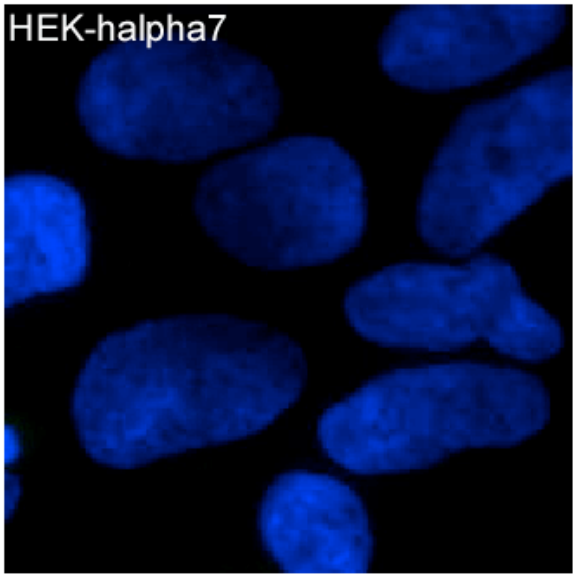
HEK-halpha7

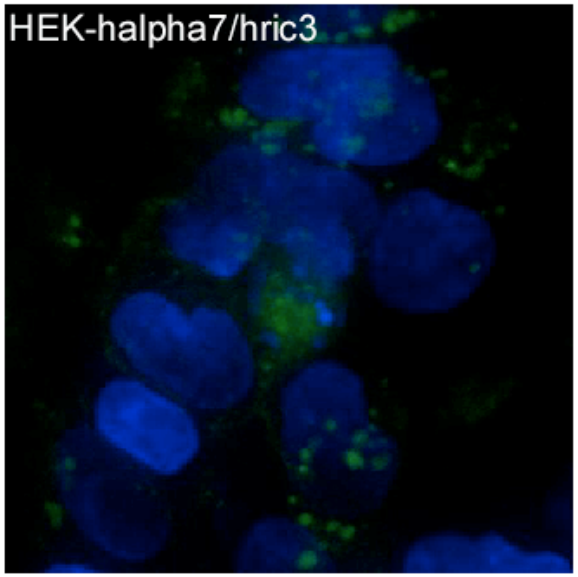
HEK-halpha7/hric3

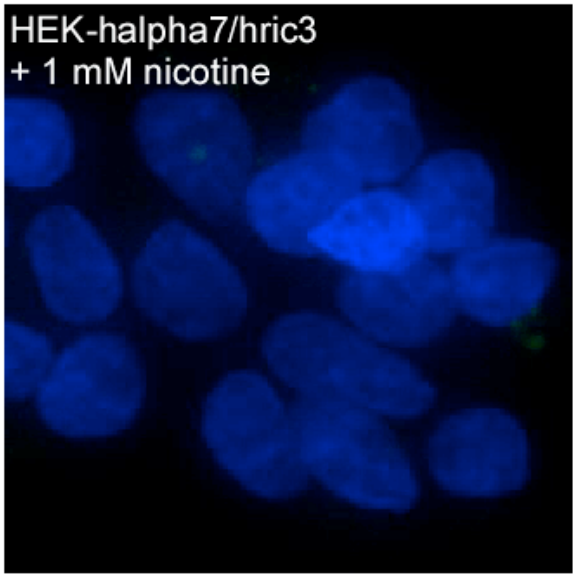
HEK-halpha7/hric3
+ 1 mM nicotine

A

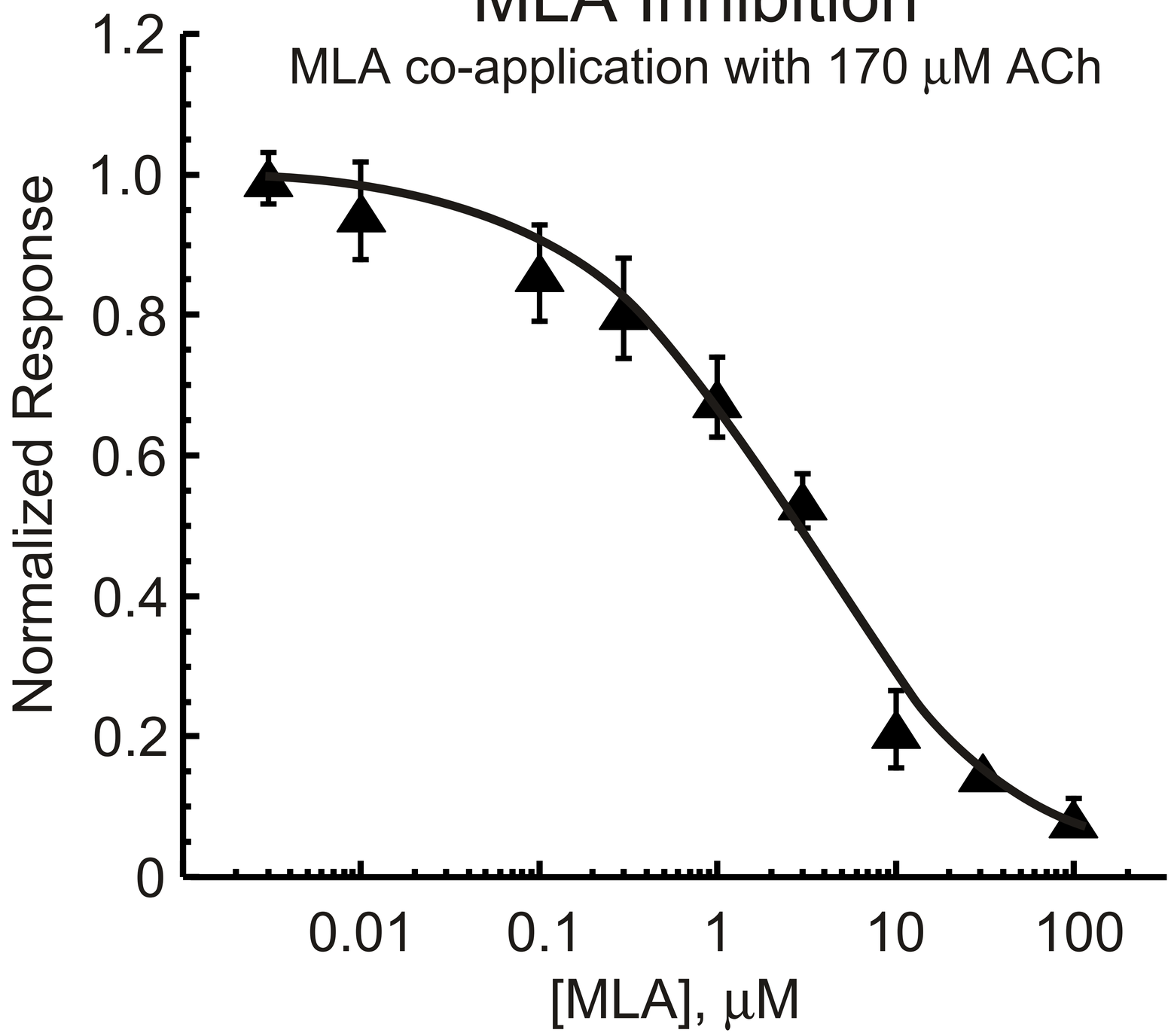
MLA Inhibition
MLA co-application with 170 μM ACh
Normalized Response
1.2
1.0
0.8
0.6
0.4
0.2
0
0.01
0.1
1
10
100
[MLA], μM

B

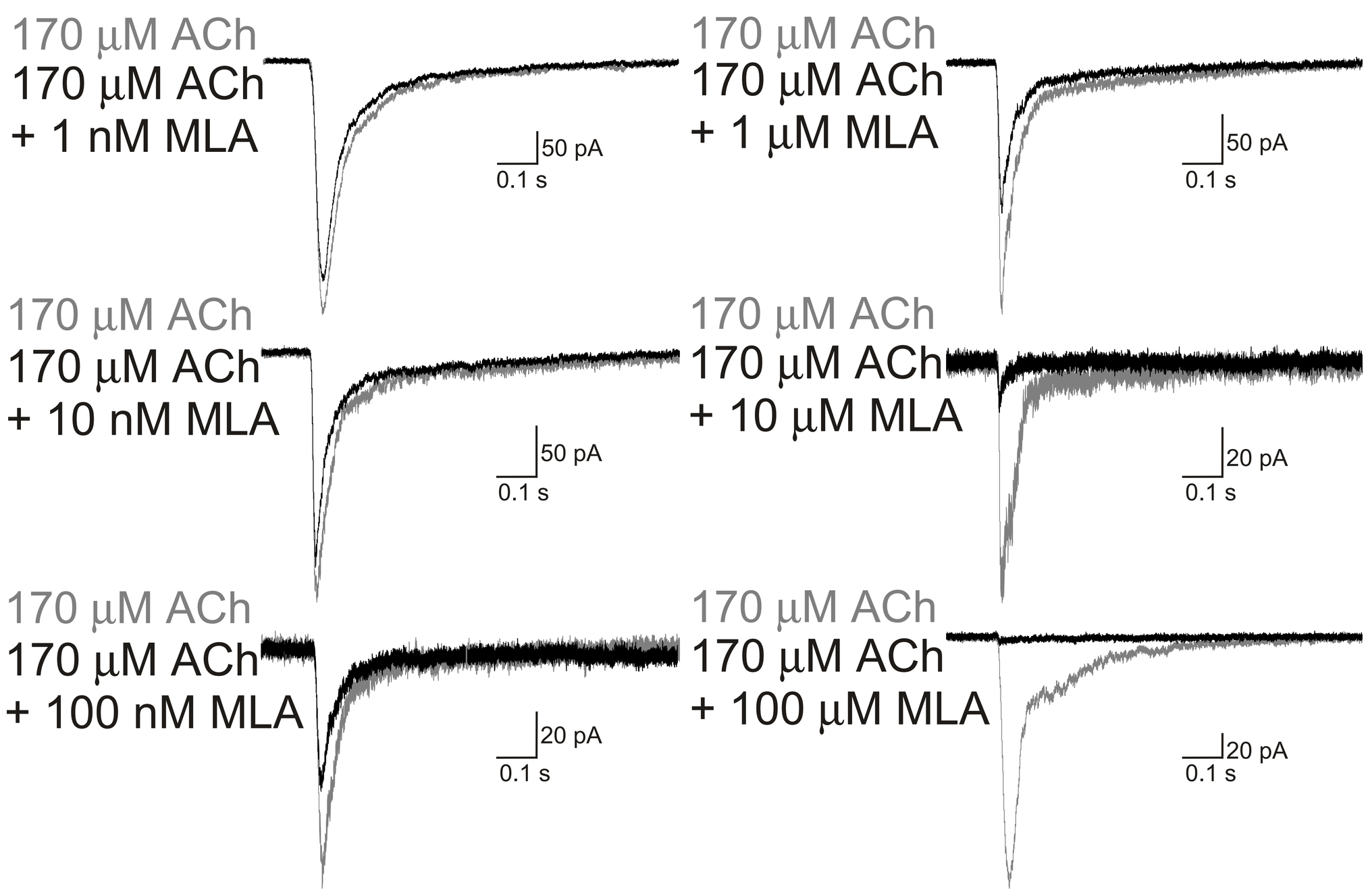
170 μM ACh
170 μM ACh
+ 1 nM MLA
50 pA
0.1 s
170 μM ACh
170 μM ACh
+ 1 μM MLA
50 pA
0.1 s
170 μM ACh
170 μM ACh
+ 10 nM MLA
50 pA
0.1 s
170 μM ACh
170 μM ACh
+ 10 μM MLA
20 pA
0.1 s
170 μM ACh
170 μM ACh
+ 100 nM MLA
20 pA
0.1 s
170 μM ACh
170 μM ACh
+ 100 μM MLA
20 pA
0.1 s

Figure 3S

Figure S4

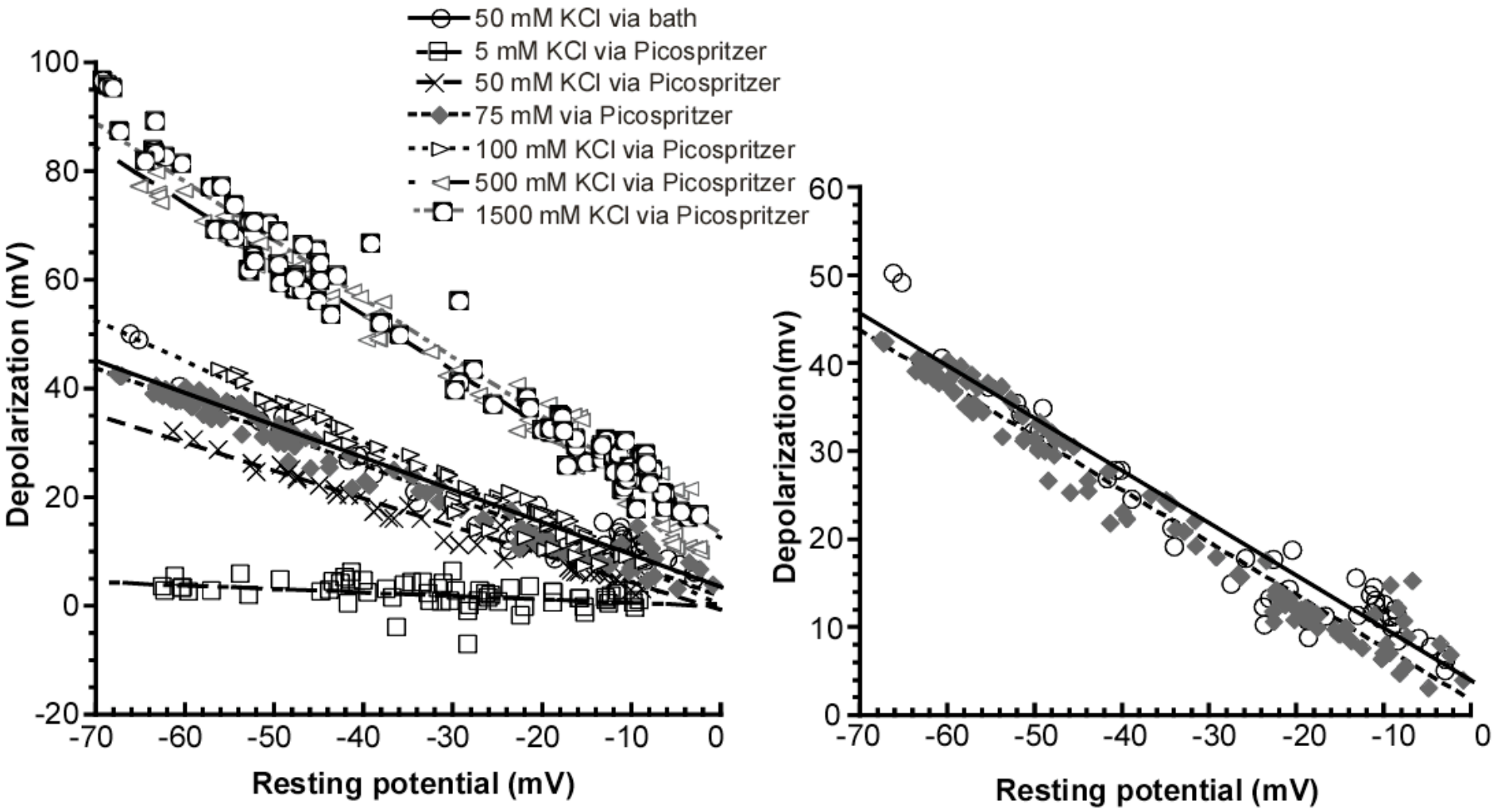
50 mM KCl via bath
5 mM KCl via Picospritzer
50 mM KCl via Picospritzer
75 mM via Picospritzer
100 mM KCl via Picospritzer
500 mM KCl via Picospritzer
1500 mM KCl via Picospritzer
Depolarization (mV)
Resting potential (mV)
Depolarization(mv)
Resting potential (mV)

Figure S5

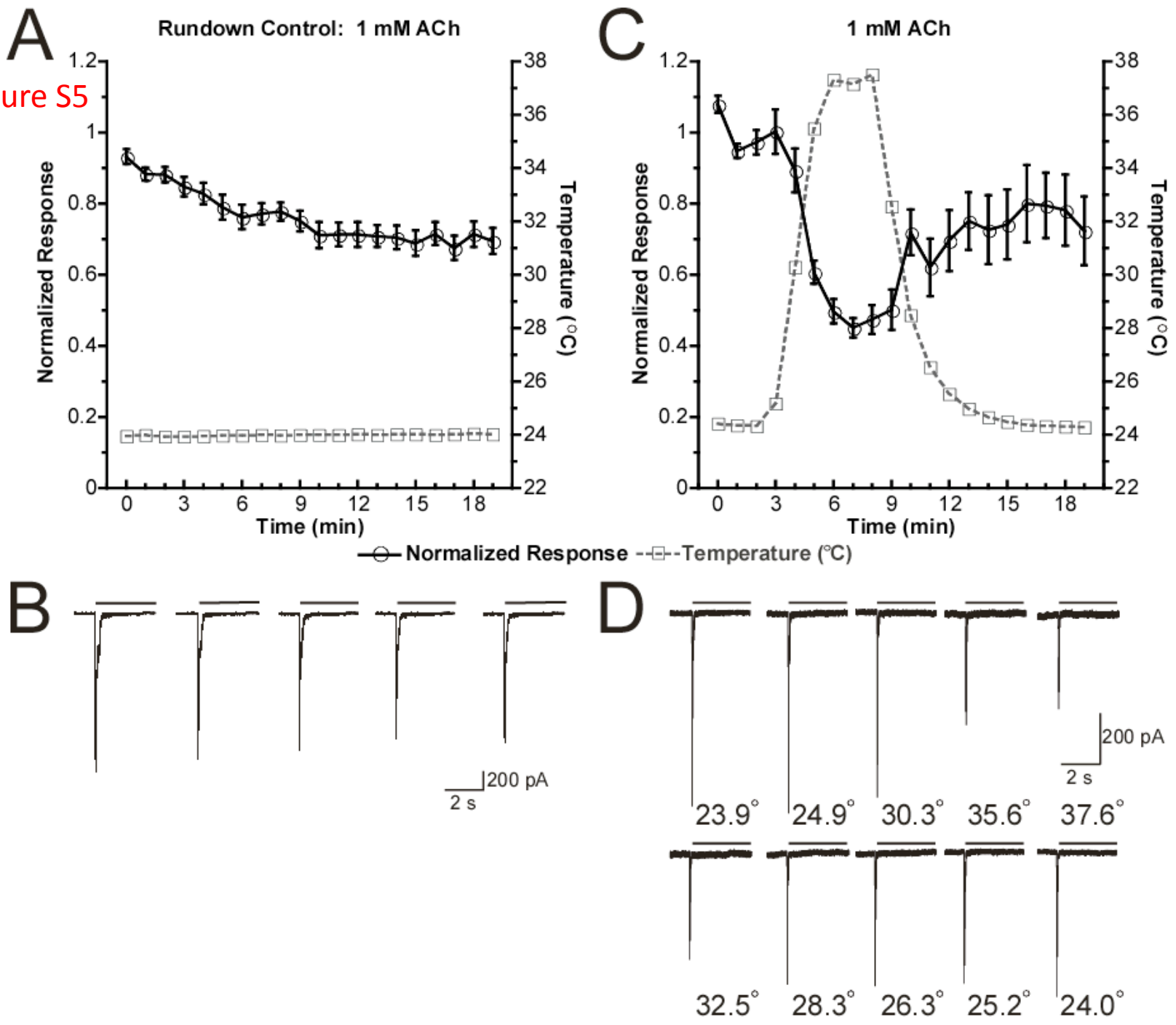
A
Rundown Control: 1 mM ACh
Normalized Response
Temperature (°C)
Time (min)
C
1 mM ACh
Normalized Response
Temperature (°C)
Time (min)
Normalized Response
Temperature (°C)
B
200 pA
2 s
D
200 pA
2 s
23.9°
24.9°
30.3°
35.6°
37.6°
32.5°
28.3°
26.3°
25.2°
24.0°

Figure S6

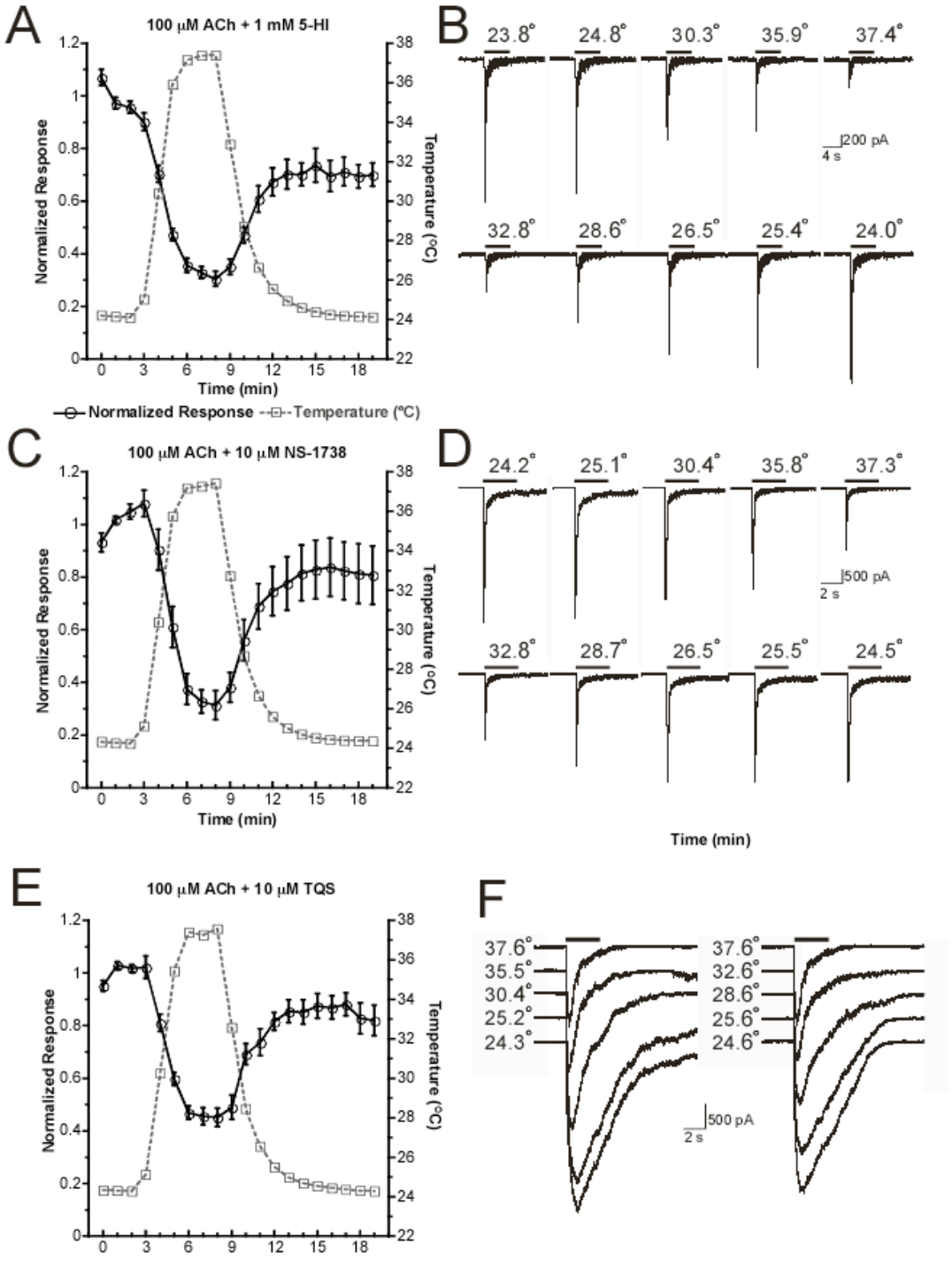
A
100 μM ACh + 1 mM 5-HI
Normalized Response
Temperature (°C)
Time (min)
Normalized Response
Temperature (°C)
B
23.8°
24.8°
30.3°
35.9°
37.4°
200 pA
4 s
32.8°
28.6°
26.5°
25.4°
24.0°
C
100 μM ACh + 10 μM NS-1738
Normalized Response
Temperature (°C)
Time (min)
D
24.2°
25.1°
30.4°
35.8°
37.3°
500 pA
2 s
32.8°
28.7°
26.5°
25.5°
24.5°
Time (min)
E
100 μM ACh + 10 μM TQS
Normalized Response
Temperature (°C)
F
37.6°
35.5°
30.4°
25.2°
24.3°
37.6°
32.6°
28.6°
25.6°
24.6°
500 pA
2 s